Shape memory effect characterization of a ternary CuAlNi high temperature SMA ribbons produced by melt spinning method

Oktay Karaduman*[1] , İskender Özkul [2] , Canan Aksu Canbay[1]

[1] Firat University, Faculty of Science, Department of Physics, Elazig, Türkiye, okinist@hotmail.com; caksu@firat.edu.tr
[2] Mersin University, Faculty of Engineering, Department of Mechanical Engineering, Mersin, Türkiye, iskender@mersin.edu.tr

Abstract

In this study, the shape memory effect characteristics of a ternary CuAlNi shape memory alloy (HTSMA) ribbons produced by melt spinning method was investigated by performing thermal and structural measurements. To investigate shape memory effect properties of the alloy ribbon some isothermal calorimetry, structural and shape recovery ratio tests were performed. The differential scanning calorimetry (DSC) test result showed the peaks of the reversible martensitic phase transformations occurred in a high temperature region (in between ~192°C - 293 °C) during the heating and cooling processes of the CuAlNi alloy ribbon. The hysteresis gap of the ribbon alloy was found narrow (20.77 °C). Some other related thermodynamical parameters parameters of the alloy were determined, too. The differential thermal analysis (DTA) measurement taken from room temperature to 900 °C revealed the sequenced multiple solid solid phase transitions in the high temperature β-phase region and this was found as compatible with the common behavior of the Cu-rich alloys. Theoretical pre-assesment on the martensite phases of the alloy was deduced from the calculated average valence electron concentration (e/a) value (1.54) of the alloy and this was proved by structural XRD test performed also in room conditions. The X-ray diffraction pattern of the alloy revealed the presence of the volumetrically dominant γ1' martensite phase over the collateral secondary β1' martensite phase in the alloy. A shape recovery performance test upon thermomechanical bending was performed on the alloy, too.

1. Introduction

Shape memory alloy (SMA) ribbons are extensively demanded due to the useful functionalities of such miniaturized SMAs in the related integrated micro-controllers and micro-electro-mechanical systems (MEMS) applications such as microactuators, microgrippers, microvalves etc. [1, 2]. Melt spinning (Figure 1) is an easy manufacturing method and by this method very thin columnar SMA ribbons with very small grain sizes can be directly obtained even without doing a further heat-treatment homogenization and quenching (rapid cooling) processes [2, 3]. Moreover, by this manufacturing method the maximal reversible strain in longitudinal direction can be increased, too [4].

The low-cost Cu-based SMAs are generally regarded as the best alternative to the most commercial NiTi SMAs with superior shape memory alloy properties but much higher costs. Plus, Cu-based SMAs have high transformation temperatures, better thermal and electrical conductivity, and also large recoverable strain [5]. As concerning to find alternative SMAs with high transformation temperatures (above 100 °C) or named as high

temperature SMAs (HTSMAs), the CuAlNi SMAs are seen the best option among the other Cu-based SMAs due to their high thermal stability [3, 4]. But the polycrystalline CuAlNi SMAs exhibit poor mechanical properties due to their brittleness caused from large grain sizes. Producing CuAlNi alloys in ribbon forms by melt spinning method is established one of the ways for grain refinement.

The transformation temperatures of SMAs are ultimately sensitive to chemical composition, even very small differences in alloying compositions can enormously change the transformation temperatures. Hence, transformation temperatures demanded in various SMA (and HTSMA) applications can be regulated by tuning alloy composition.

In this work, the ternary CuAlNi HTSMA ribbons were manufactured by melt spinning method. Without doing any further heat-treatement and quenching procedures on the ribbon alloy, the shape memory effect characterization was made by thermostructural DSC, DTA and XRD tests and thermo-mechanical shape recovery performance test on the alloy ribbon was also carried out.
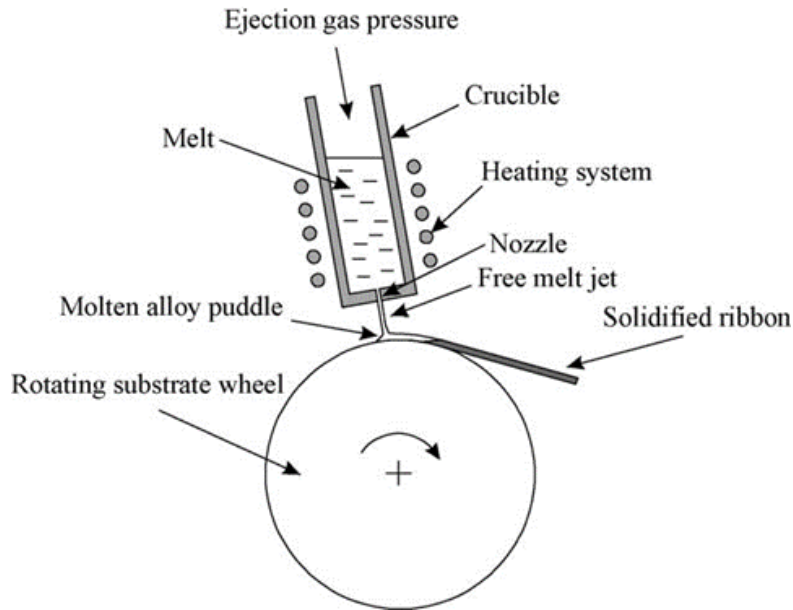
Figure 1. Schematic illustration of a free jet melt spinner [3]

2. Method

The CuAlNi SMA ribbons with a new alloy composition of 71.08Cu-25.04Al-3.88Ni (at%) or 82.5Cu-12.34Al-4.16Ni (wt%) were fabricated by melt spinning method. In this process, at first, the powders of the alloying Cu, Al, and Ni elements with high purity (%99.99) were mixed and then the pellet forms of this powder mixture were obtained by applying pressure. Then the pellets were melted via melt spinning procedure by using an Edmund Buehler melt spinner system in argon atmosphere to prevent oxidation of alloy ribbons. Thus, the CuAlNi alloy ribbons with 15 μm thickness and ~5 mm width was successfully produced. The test specimens of the obtained melt spun alloy ribbons were prepared by cutting them properly for the measurements. A Shimadzu 60A label DSC instrument was utilized for performing the DSC test taken at a single heating/cooling rate of 25 °C/min under 100 ml/min constant argon gas flow. Under same gas flow and also at a single 25 °C/min of heating/cooling rate, the cyclical DTA test was carried out by using a Shimadzu DTG-60AH system in between room temperature and 900 °C. The shape recovery performance test of the alloy ribbon upon bending load was performed and the shape recovery ratio between the deformed martensitic shape (storage state, S) of ribbon and the recovered austenitic shape (recovery state, R) formed by applied heat on the deformed ribbon was calculated by using the determined position angles of two shape states. The alloy composition was detected by a Zeiss Evo MA10 model EDX equipment under room conditions. By using CuKα radiation the X-ray diffraction (XRD) test made at room temperature by using a Rigaku RadB-DMAX II diffractomer displayed the diffraction peaks planes reflected from the atomic crystal planes of the martensite structures at room temperature.

3. Results

The thermocyclical DSC test result of the CuAlNi ribbon obtained at a single heating/cooling rate of 25 °C/min is given as graphic of DSC heat flow (mW) versus temperature (°C) axis in Figure 2-a, and the same graphic drawn out on time axis in Figure 2-b. As seen on the both version of the DSC graphic, the correspondent up-exo (on cooling) and down-endo (on heating) peaks observed at between ~192 °C and ~293 °C indicates the backward austenite to martensite (A→M) and forward martensite to austenite (M→A) phase transformations, respectively.
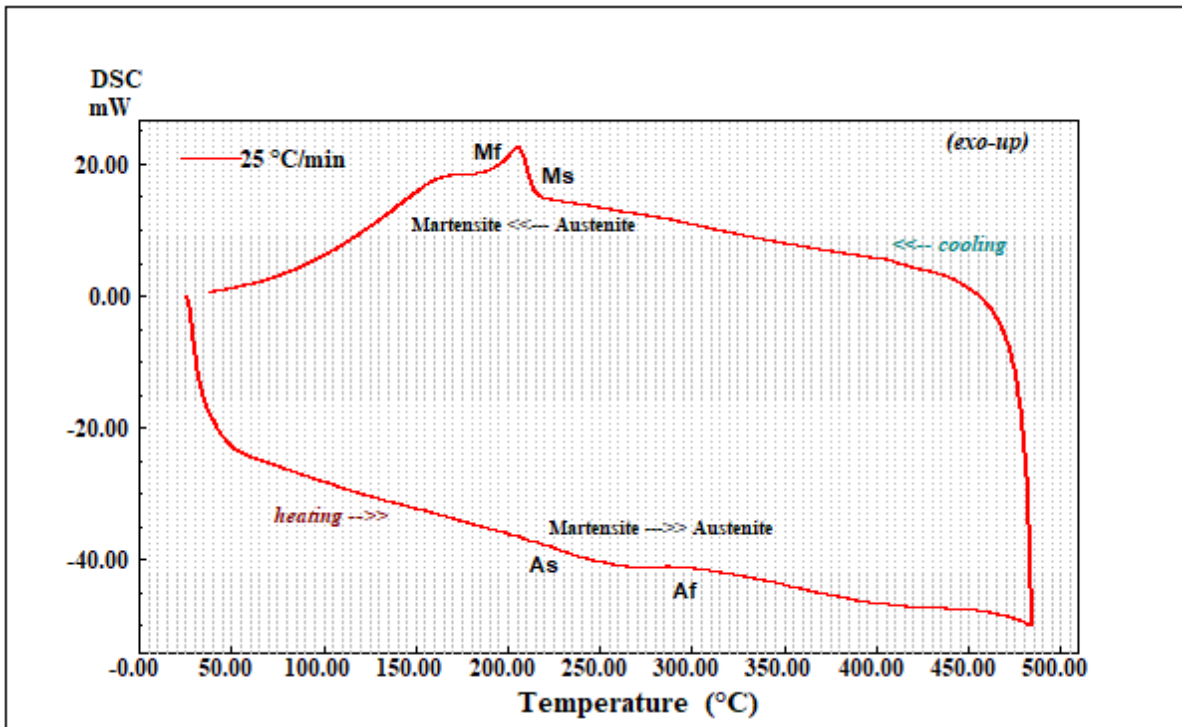
(a)
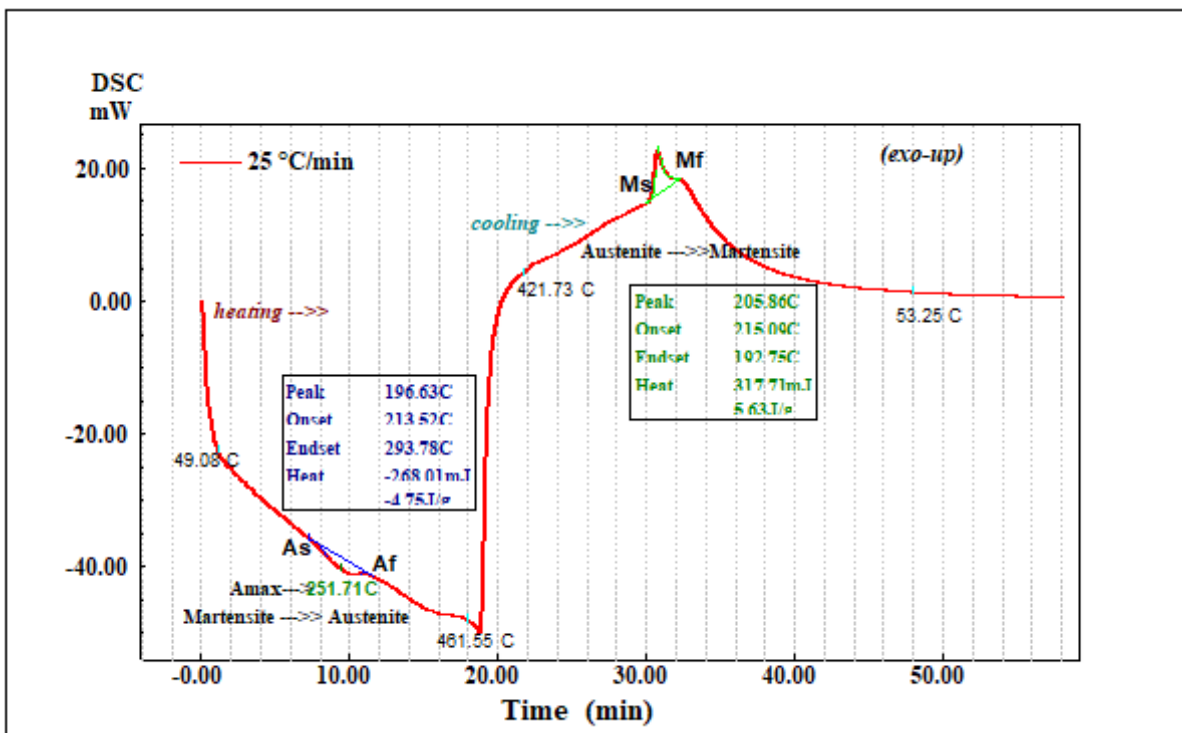
(b)

Figure 2. The DSC test result of the produced CuAlNi SMA ribbon; a) the DSC heating/cooling curve (thermogram) cycled on temperature axis, b) the same DSC curve drawn out on time axis and with data insets of the analysed forward and backward martensitic transformation peaks. In these peak analysis data insets, which were automatically inserted by DSC analyser program applying tangent method on the selected area of a peak, the onset temperatures are the phase start temperatures (A_s and M_s), the endset temperatures are phase finish temperatures (A_f and M_f) and the enthalpy change values (J/g) as integral of transformation peak areas were also directly given at the bottom of these data insets.

For this reversible martensitic transformation, the characteristic phase start and finish temperatures (A_s, A_f, M_s, and M_f), the maximum temperature M→A peak (A_{max}) (actually here this is the minimum in the case of endo-peaks seen in the tests made by Shimadzu DSC instrument), the hysteresis gap (A_s-M_f), the equilibrium temperature (T_0), the enthalphy ($\Delta H_{M \to A}$) and entropy ($\Delta S_{M \to A}$) change amounts for M→A transformations were obtained and tabulated in Table 1.

Table 1. The charactersistic martensitic transformation temperatures and some related kinetic parameters of the CuAlNi HTSMA ribbon.

Heating/cooling rate (°C/min)	A_s (°C)	A_f (°C)	A_{max} (°C)	M_s (°C)	M_f (°C)	A_s-M_f (°C)	T_0 (°C)	$\Delta H_{M \to A}$ (J/g)	$\Delta S_{M \to A}$ (J/g°C)
25	213.52	293.78	251.71	215.09	192.75	20.77	254.44	4.75	0.01867

Apart from the DSC result, an emprical formula (Equation 1) [4] is given for making an estimation of the M_s temperature of CuAlNi alloys;

$$M_s(°C) = 2020 - [134 \times (wt.\%Al)] - [45 \times (wt.\%Ni)] \tag{1}$$

By substituting the mass percentage (wt.%) values of Al and Ni alloying elements in the Equation 1, the M_s temperature of the produced CuAlNi HTSMA ribbon was found as 179.24 °C and this value was found close to the M_s value (215.09 °C) determined by DSC analysis (given in Table 1). The reason of the difference between these two M_s values may be caused from the DSC test and the cooling rate or the presence of small local composition diversities in the ribbon alloy (without making post heat treatment and quenching after melt spinning, some hypoeutectical precipitations may be remained in the alloy ribbons, and this is going to be shown in the XRD result section ahead).

The equilibrium temperature (T_0) is an important kinetic parameter for SMAs. It is the temperature at where the chemical Gibbs free energy (G) values of two austenite and martensite phases are balanced, meaning that at this temperature there is zero driving force can trigger the alloy to make transform to any one of the two opposite phases [6]. By using $T_0=0.5 \times (A_f+M_s)$ formula [6] the T_0 value of the ribbon alloy was found as given in Table 1. The entropy change ($\Delta S_{M \to A}$) of the endothermic M→A transformation was found by using $\Delta S_{M \to A} = \Delta H_{M \to A}/T_0$ relation [6, 7].

The DTA cyclic curve of the CuAlNi alloy ribbon obtained at the single running heating/cooling rate of 25 °C/min is presented in Fig.3. According to this figure, on the heating fragment of the DTA curve, the appeared sequential peaks indicated the multiple phase transformations of **"B1**(austenite, L2$_1$)→**B2**(metastable)→precipitating(α+γ2)→**eutectoid** recomposition (of the precipitates)→**B2**(ordered)→**A2**(disordered)"throughout of the high temperature β-phase region, which is a common behavior of Cu-based alloys. [6, 7].

The average valence electron concentration per atom (e/a) value of Cu-based SMAs can give some pre-knowledge about the formed martensite phases with their volumetric comparison in those alloys. By using $e/a=\sum f_i v_i$ formula [7], where f_i is the each atomic fraction (at.%) of the alloying elements and v_i represents the corresponding valence electron numbers of these elements. This e/a value found higher than 1.49 implies that the hexagonal γ1'(2H) martensite phase should have dominantly formed in the alloy over monoclinical β1'(M18R) martensite phase [6, 7]. This theoretical prediction is to be proved by the result of structural X-ray diffraction test performed on the alloy ribbon as given in Figure 4.

The XRD pattern of the alloy ribbon is given in Fig.4. The highest γ1'(211) martensite peak seen on this X-ray diffraction pattern shows a little dominancy of this martensite phase over the β1' martensite, and this affirms the prediction made by e/a value of the alloy ribbon. The other observed peaks on the XRD pattern are some other martensite phases of γ1' and β1', β1, and precipitates of γ1, γ2, and αCu [5, 8-15]. These complex and short peaks including many small precipitation peaks indicate the high polycrystalline nature of the alloy ribbon matrix. This was also caused because of not making a post-heat-treatment after melt spinning process.

The thermomechanical bending test upon loading, unloading and recovering by heat was performed to test the shape memory recovery ratio (η) value of the ribbon alloy. The images of this test is given in Figure 5-a and Figure 5–b. A formula [16]to calculate the shape recovery ratio (η) is given in Equation 2;

$$\eta = \frac{\theta_R}{180 - \theta_e} \times 100 \tag{2}$$

where; θ_e is the angle (determined as ~20°, in Figure 5-b) in between loaded bending and unloaded plastically deformed (martensite) shape position, and θ_R angle (determined as ~50°, in Figure 5-b) between the unloaded shape position and original shape (R, recovery) position of the alloy ribbon. Thus, the shape recovery ratio (η) of the melt spun CuAlNi HTSMA ribbon was found as ~%31.25 this value could be enhanced more by optimizing test conditions. Also, the alloy ribbon was tended to fracture very much during the bending process, mostly because of its very small thickness.
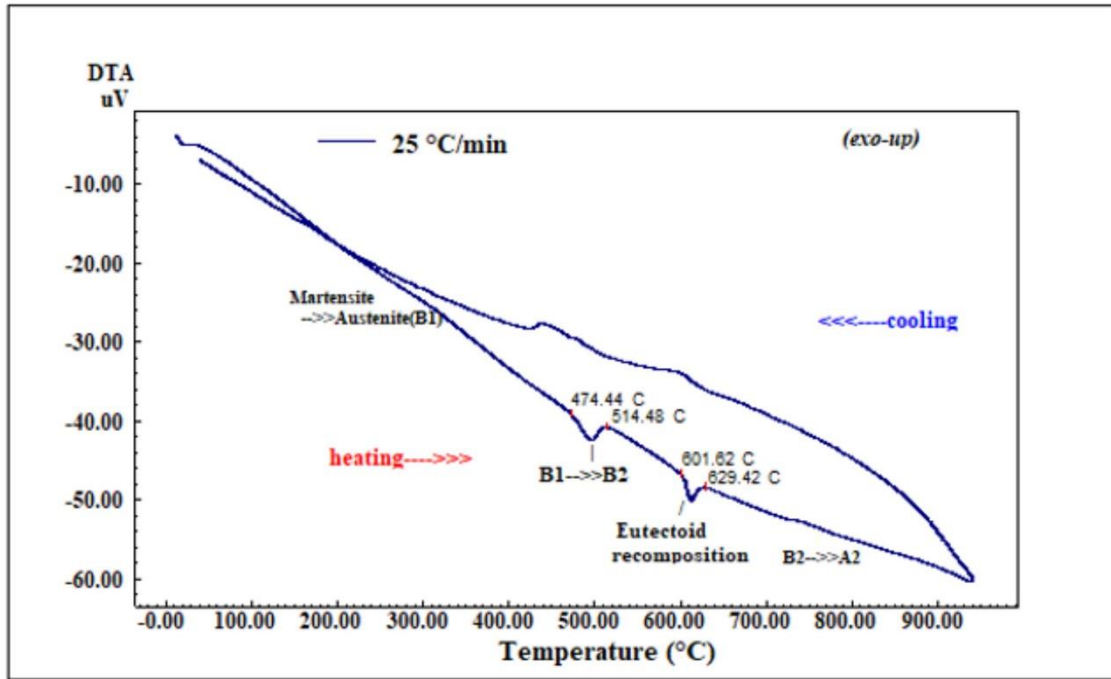
Figure 3. The cyclic DTA heating/cooling curve of the CuAlNi SMA ribbon displays the multiple phase transformations of "B1(austenite, L2₁) →B2(metastable)→precipitating(α+γ2) →eutectoid recomposition (of the precipitates) →B2(ordered) →A2 (disordered)" throughout of its high temperature β-phase region, which is a common behaviour of Cu-based alloys.
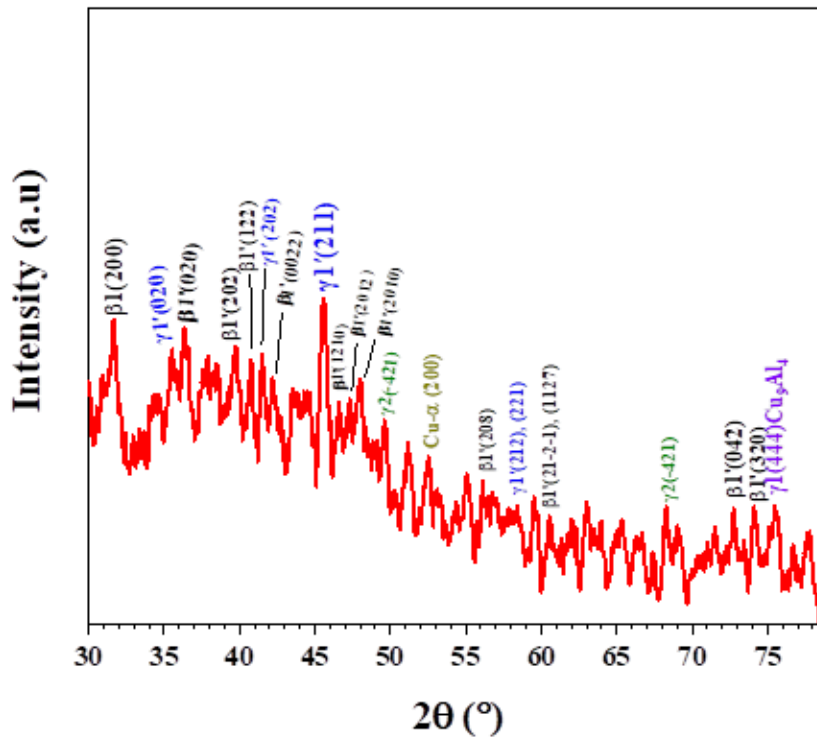
Figure 4. The XRD test result of the produced CuAlNi HTSMA ribbon. The main γ1'(211) martensite peak seen on this X-ray diffraction pattern shows the dominancy of this martensite phase over the β1' martensite.

(a)

(b)
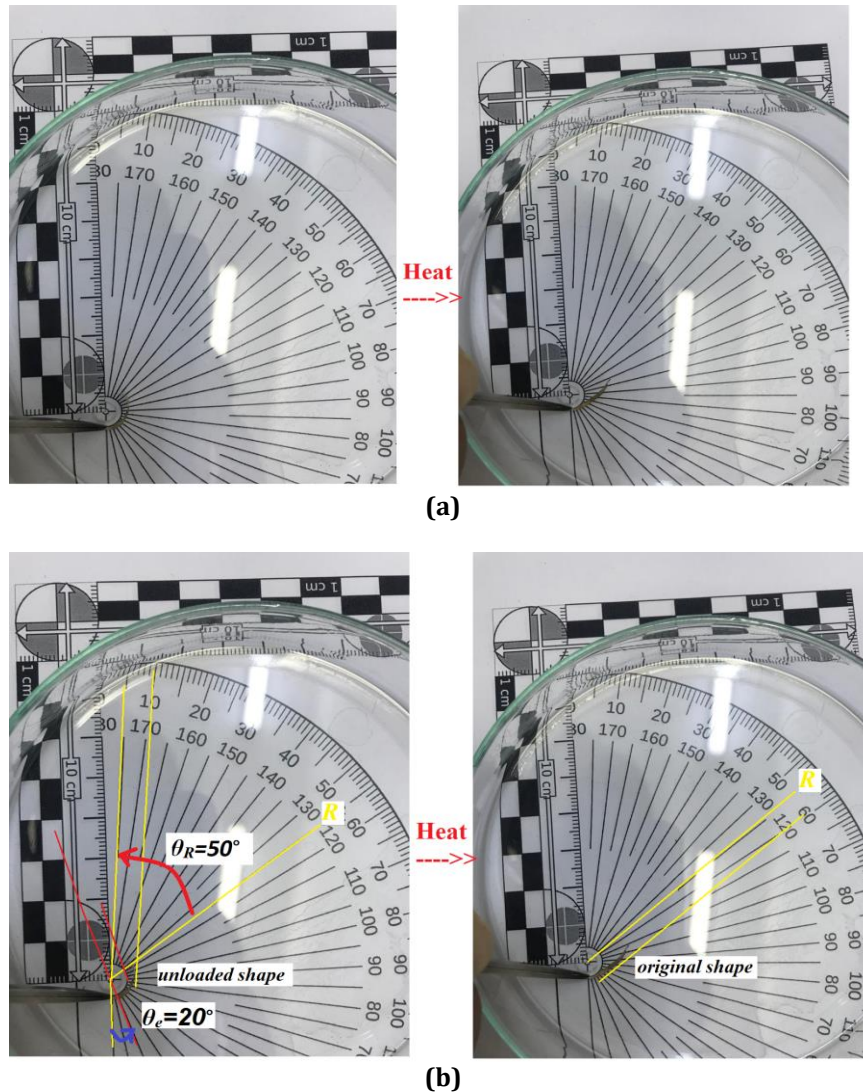
Figure 5. The shape recovery performance test of the CuAlNi HTSMA ribbon. a) as pictures of unloaded ribbon in deformed martensite state and after recovery induced by heat, b) same pictures with determined θ_e angle between the loaded and unloaded (plastically-deformed) martensite shapes' positions and θ_R angle between unloaded shape position and original austenite shape (R, recovery) position.

4. Conclusion

In this work, the CuAlNi HTSMA ribbons with 15 micrometer thickness were successfully manufactured by melt spinning method. The shape memory effect characterization of HTSMA ribbon was implemented by performing thermal DSC/DTA, structural XRD tests, the shape recovery performance of the alloy was tested by making thermo-mechanical bending test. The DSC test showed the alloy ribbon having a shape memory effect property based on the martensitic phase transformation occurred at between ~192 °C and ~293 °C and this range. The DTA test revealed the alloy ribbon's behaviour in high temperature β-phase region as compatible with the common behaviour of the Cu-based alloys. The XRD peaks showed the polycrystalline structure of the alloy including the dominat hexagonal 2H martensite phase in the alloy ribbon at room temperature. The shape recovery ratio of the melt spun CuAlNi HTSMA ribbon tested by thermomechanical bending was found as ~%31.25, which can be optimized. In conclusion, this melt spun HTSMA ribbon with a new composition may be used in various miniaturized HTSMA applications such as thermo-electro-mechanical systems, microactuators and related applications.

Author contributions

Oktay Karaduman: Conceptualization, Methodology, Software **İskender Özkul:** Data curation, Writing-Original draft preparation, Software, Validation. **Canan Aksu Canbay:** Visualization, Investigation, Writing-Reviewing and Editing.

Conflicts of interest

The authors declare no conflicts of interest.

References

1. Jani, J. M., Leary, M., Subic, A., & Gibson, M. A. (2014). A review of shape memory alloy research, applications and opportunities. *Materials & Design (1980-2015), 56*, 1078-1113.
2. López Cuellar, E., López Pavón, L., Nuñez Mendoza, E., Araújo, C. J. D., Castro, W. B. D., Gonzalez, C., & Otubo, J. (2016). Effect of spun velocities and composition on the microstructure and transformation temperatures of TiNi shape memory ribbons. *Materials Research, 19*(5), 1132-1137.
3. Font, J., Cesari, E., Muntasell, J., & Pons, J. (2003). Thermomechanical cycling in Cu–Al–Ni-based melt-spun shape-memory ribbons. *Materials Science and Engineering: A, 354*(1-2), 207-211.
4. Lojen, G., Anžel, I., Kneißl, A., Križman, A., Unterweger, E., Kosec, B., & Bizjak, M. (2005). Microstructure of rapidly solidified Cu–Al–Ni shape memory alloy ribbons. *Journal of Materials Processing Technology, 162*, 220-229.
5. Matlakhova, L. A., Pereira, E. C., Pulnev, S. A., Shigue, C. Y., & Palii, N. A. (2020). Physical and Structural Characterization of Monocrystalline Cu-13.7% Al-4.2% Ni alloy submitted to Thermo-Cyclical Treatments under Applied Loads. *Metals, 10*(2), 219.
6. Canbay, C. A., Karaduman, O., Ünlü, N., Baiz, S. A., & Özkul, İ. (2019). Heat treatment and quenching media effects on the thermodynamical, thermoelastical and structural characteristics of a new Cu-based quaternary shape memory alloy. *Composites Part B: Engineering, 174*, 106940.
7. Canbay, C. A., & Karaduman, O. (2021). The photo response properties of shape memory alloy thin film based photodiode. *Journal of Molecular Structure, 1235*, 130263.
8. Braga, F. d. O., Matlakhov, A. N., Matlakhova, L. A., Monteiro, S. N., & Araújo, C. J. d. (2017). Martensitic transformation under compression of a plasma processed polycrystalline shape memory CuAlNi alloy. *Materials Research, 20*(6), 1579-1592.
9. Saud, S. N., Hamzah, E., Abubakar, T., & Bakhsheshi-Rad, H. (2015). Thermal aging behavior in Cu–Al–Ni–xCo shape memory alloys. *Journal of Thermal Analysis and Calorimetry, 119*(2), 1273-1284.
10. Bilican, D., Kurdi, S., Zhu, Y., Solsona, P., Pellicer, E., Barber, Z. H., . . . Fornell, J. (2019). Epitaxial versus polycrystalline shape memory Cu-Al-Ni thin films. *Coatings, 9*(5), 308.
11. Najib, A. S. M., Saud, S. N., & Hamzah, E. (2019). Corrosion Behavior of Cu–Al–Ni–xCo Shape Memory Alloys Coupled with Low-Carbon Steel for Civil Engineering Applications. *Journal of Bio-and Tribo-Corrosion, 5*(2), 47.
12. Zhang, X. & Q.-S. Liu, *Influence of alloying element addition on Cu–Al–Ni high-temperature shape memory alloy without second phase formation.* Acta Metallurgica Sinica (English Letters), 2016. **29**(9): p. 884-888.
13. Chentouf, S., Bouabdallah, M., Gachon, J., Patoor, E., & Sari, A. (2009). Microstructural and thermodynamic study of hypoeutectoidal Cu–Al–Ni shape memory alloys. *Journal of Alloys and Compounds, 470*(1-2), 507-514.
14. Canbay, C.A., O. Karaduman, & İ. Özkul, *Investigation of varied quenching media effects on the thermodynamical and structural features of a thermally aged CuAlFeMn HTSMA.* Physica B: Condensed Matter, 2019. **557**: p. 117-125.

15. Saud, S. N., Hamzah, E., Abubakar, T., & Bakhsheshi-Rad, H. (2015). Thermal aging behavior in Cu–Al–Ni–xCo shape memory alloys. *Journal of Thermal Analysis and Calorimetry, 119*(2), 1273-1284.
16. Jiao, Y., Wen, Y., Li, N., He, J., & Teng, J. (2010). Effect of solution treatment on damping capacity and shape memory effect of a CuAlMn alloy. *Journal of Alloys and Compounds, 491*(1-2), 627-630.